Experimental investigation of a radiative heat pipe for waste heat recovery in a ceramics kiln

Bertrand Delpech, Brian Axcell, Hussam Jouhara*

College of Engineering, Design and Physical Sciences, Brunel University London, UB8 3PH, UK

A B S T R A C T

Following the energy crisis in the 1980s, energy-saving technologies have been investigated and implemented in order to decrease the energy consumption and greenhouse gas emissions of major industrial sectors such as metals, ceramics and concrete. The ceramics industry is still, in Europe, one of the major energy consuming manufacturing processes. Hence energy saving solutions have been investigated in order to decrease the energy consumption of the manufacturing process. The main energy-consuming process is the firing stage with more than 50% of all of the energy required for the process. The energy used during the firing stage is then released during the cooling stage. To improve the heat recovered during the cooling stage, a radiative heat pipe ceiling has been investigated. The heat recovered during the cooling stage is then sent to the drying stage. The proposed system is composed of a radiative heat pipe, a kiln and a ceramics heater. The radiative heat pipe is made of ten parallel pipes of 28 mm diameter and a wall thickness of 2 mm the tubes are connected at the bottom by a 28 mm pipe and a condenser section of 50 mm the condenser is a shell and tube system with 9 pipes of 10 mm. The system was cooled by water. The radiative heat pipe has been tested at different flow rate and ceramics heater temperature. The experimental results shown that the radiative heat pipe was able to recover heat using radiation and natural convection in an enclosed kiln. The system was able to recover up to 4 kW. This paper describes this innovative solution for recovering heat from the cooling stage of an earth roller kiln for tile ceramics manufacturing, transformed into hot clean air for the drying stage of the ceramics manufacturing process.

© 2018 Elsevier Ltd. All rights reserved.

1. Introduction

Energy savings research programme in Europe has been growing important over the year. The EU commission has set a target to reduce greenhouse gas emissions by 80–95% in 2050. In order to match this target, research in waste heat recovery in industrial setting is currently widely investigated [1]. Waste heat recovery in industry became over the year a strategic subject for research in environmental and process optimization. 70% of the energy required in the industry is related to heating, this heating results in significant amount of heat lost, up to 50% [2]. The ceramics industry is one of the largest consumers of energy in the industrial sector; more than 30% of the production cost of ceramic goods is related to the energy input in the manufacturing process. The ceramics sector was in 2016 the second most energy intensive manufacturing process in Europe with a consumption of almost 1.67 MWh [3]. The ceramics industry can be divided into two sectors. The advanced or technical ceramics sector applies to electronics, security and healthcare. In these fields, the chemical and physical properties of the ceramics, made of chemically prepared powders, are controlled completely. The complexity of this manufacturing process makes advanced ceramics more expensive than with traditional manufacturing processes. The traditional ceramic process is the biggest sector regarding the amount of ceramics products produced, the energy consumed and the total amount of trade. The sector can be separated into six different applications, wall and floor tiles, brick roof tiles and pipes, refractories, sanitary ware, table and ornamental ware, and abrasive ceramics (see Fig. 1).

The manufacturing process of traditional ceramics is quite similar for each product (see Fig. 2). The first stage is the preparation and shaping of the clay, followed by the drying stage, the firing stage where most of the energy is used to heat the clay up to

---

<div style="border:1px solid">

Nomenclature

	σ Stephan-Boltzmann constant $= 5.67 \times 10^{-8}$ W/m$^2K^4$

Symbols

A	Surface area (m^2)
d	Pipe diameter (m)
E	Emitted heat by surface area (W/m^2)
F	View factor for radiation heat transfer
h	Heat transfer coefficient (W/m^2)
J	Radiosity, radiation leave surface area (W/m^2)
k	Thermal conductivity (W/m^2.K)
Q	Heat transfer rate (W)
R	Thermal resistance (K/W)
Ra	Rayleigh number
T	Temperature (K)

Greek letters

ε	Emissivity

Subscripts

c	Condenser
ci	Condenser inner side
co	Condenser outer side
$cond$	Conduction
$cold$	Coolant, water
e	Evaporator
ei	Evaporator inner side
eo	Evaporator outer side
H	Heaters
HP	Heat pipe
rad	Radiation
v	Vapour
W	wall

</div>

1300 °C depending on the product and kiln technology, and the cooling stage where the tiles are cooled to ambient temperature before packaging and shipping [4]. Of the seven applications, wall and floor tiles represent the largest. The wall and floor tiles application group's items used to cover roofs, walls, showers and any decoration materials. The tile sector represents a market of 14 billion euros and consumes 75% of the total energy consumed within the traditional sector [5]. The firing stage is the main energy consumer in the manufacturing process. The earth roller kiln is the most commonly used technology. The main purpose of the firing stage is to bind the molecules of the tiles to increase the mechanical properties. Four stages can be identified in the firing process. First the tiles are heated to 1300 °C, then the tiles are quickly cooled down to 700 °C using a directed air stream. Next indirect cooling is used to cool down the tiles uniformly during the creation of the quartz crystals. Finally, the tiles are slowly cooled down from

300 °C to ambient temperature using air. The main challenges in the roller kiln and in the tile ceramics sector generally is to recover the heat efficiently from the cooling section.

The temperatures of the tiles are quite high and heat cannot be recovered using traditional heat exchangers. Hence heat pipe technology has been applied to a lab-scale kiln using remote cooling.

Several studies have been made on waste heat recovery in the ceramics industry.

Heat pipe systems have been developed in industrial applications over the past few year. A heat pipe is a system that is able to transfer large amounts of heat through a pipe without any mechanical part. Heat pipe systems are widely applied on electronics using the wick technology in order to transfer the working fluid from the condenser to the evaporator. The thermosiphon heat pipe used in this study relies on the evaporation and condensation of a working fluid contained in a shell.

A heat pipe is composed of 3 sections, the evaporator section where the heat is input into the heat pipe. The working fluid inside the pipe will boil and change phase into saturated vapour. This saturated steam will travel upwards through the adiabatic section to the condenser section. The working fluid will release the latent heat to the heat sink, hence the working fluid will travel back to the evaporator. The cycle will then start again (Fig. 3). The heat pipe system has multiple benefits such as an isothermal operation by avoiding any cold spots and condensation risk, which will increase the life time of the system. The heat pipe is considered as a passive device as no pumping/mechanical components are needed to send the condensed working fluid back to the evaporator. The reactivity of heat pipe is higher than other heat transfer system, which offers different control options.

2. Literature review

Most of the research has focused on the drying stage, as it is the second most energy consuming stage in the process. Most of the studies have been reviewed by Ref. [5]. The optimization of the recirculation of the drying air in the chamber has been investigated. The energy saving has been improved by using more sophisticated ventilation techniques that will take into account different parameters such as relative humidity, temperature and flow rate. Another optimization was the use of the hot air coming from the cooling section of the kiln to improve the energy balance of the
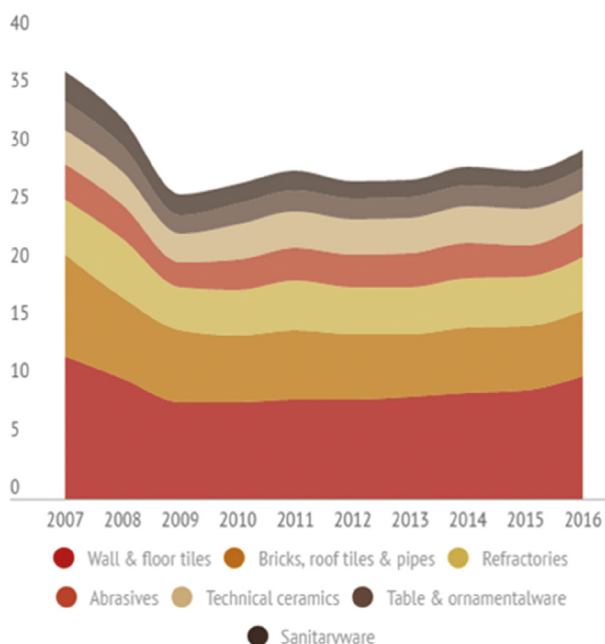

Fig. 1. 2016 ceramic industry production (in bilion Euros) [3].
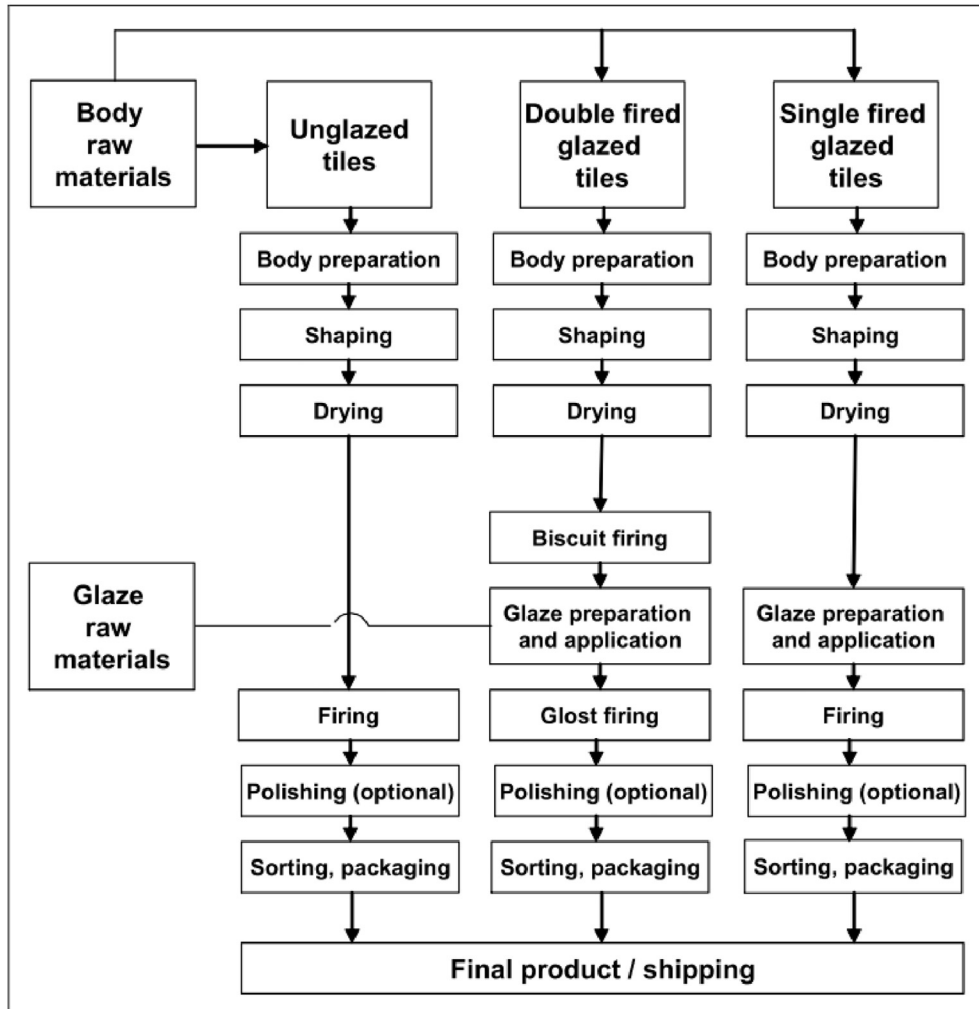
Fig. 2. Tiles manufacturing process [4].

drying section. The main issues with this development is the use of flue gas in the dryer. Pulsed hot air has also been investigated. Instead of a constant airflow in the dryer, the air is blasted periodically in the chamber which will allow a higher drying temperature. By using pulsed hot air, the drying has been reduced by 40 min compared to the classic roller dryer. Microwave drying techniques have also been developed. The microwaves have two main advantages, first, only the object is heated instead of the surrounding air. The second advantage is that not only the surface of the body is heated but also the centre of the body. This allows the moisture to travel from the centre of the body to the surface. Microwave drying can significantly decrease the drying time of the tile manufacturing process thus allowing a higher efficiency of the process [6]. An Organic Rankine Cycle applied to the ceramics has also been investigated by *Peris* et al. [7] (see Fig. 4). The ORC has been proven to be able to recover heat at a large range of temperatures, that is, low grade and high grade heat. The ORC system, similar to the Rankine cycle, is composed of an evaporator, an expander and a regenerator.

The system has been implemented in a typical year of production. The results have shown a total heat recovery of 115 MWh for the whole year. The system could potentially recover about 240 MWh of primary energy for a year, which represent 31 tonnes

per year of CO$_2$. The payback of the system is 4–5 years.

Systems to recover heat from the cooling section have been investigated by *Mezquita* et al. [8]. The flue gas from the cooling section goes through a heat exchanger (see Fig. 5). The heat recovered by the heat exchanger is then used to feed the burner and the drying stage. The application of this technology is limited due to the condensation of acidic gases and the development of fouling on the heat exchanger.

A cogeneration system has also been developed for the ceramics industry. The proposed system, developed by *Beltran* [9], is shown in Fig. 6. Fresh air from the factory is injected into the system, the air is then mixed with the hot air coming from the cooling section of the kiln and the hot air coming from the cogeneration system. If the temperature is not high enough, a burner will heat up the air to the desired temperature and, using this process, the potential energy saving is 10%–50% of the energy used in the drying stage [10].

Heat pipe technology has been applied in the ceramics industry by *Delpech* et al. [11]. The system consists of a heat pipe heat exchanger system looking at the exhaust of the cooling section. The heat recovered from the heat pipe is then sent to the dryer. This paper shows the benefit of the heat pipe system compared to classical heat exchanger systems. The heat recovered from the cooling section was larger than for a classical heat exchanger and
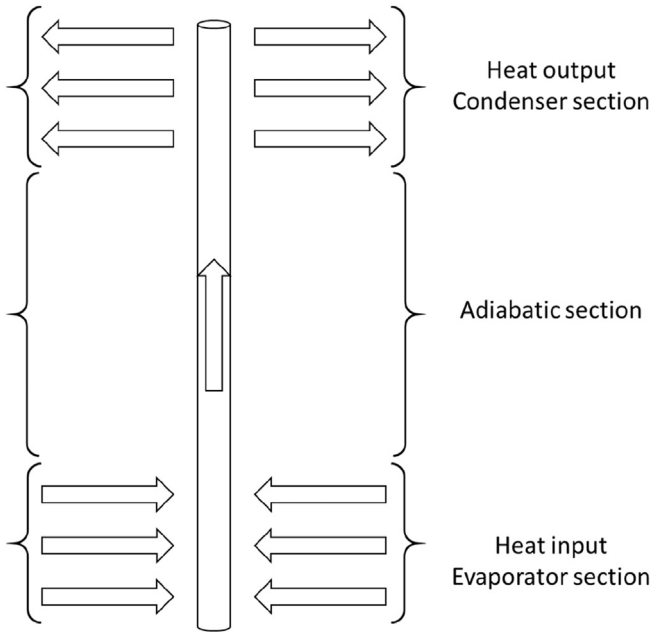
Fig. 3. Schematic heat pipe principle.

fouling was avoided due to the design of the heat pipe system. The simulation has shown a potential heat recovery of more than 800 MWh of thermal energy per year.

Radiative heat pipe technology has also been developed in the steel industry by *Jouahra* et al. [12]. The flat heat pipe system composed of a bundle of tubes connected by a collector and a condenser section was exposed to a moving line of hot steel wires. The heat was extracted through the condenser section, consisting of a bundle of tubes, with water as a heat sink. The heat recovered from a heat pipe area of one square meter was 15.6 kW at a water flow rate of 0.38 kg/s and a heat source at 450 °C. The radiative pipe technology was also developed for a solar application by *Jouhara* et al. [13]. The heat pipe was composed of a bundle of channels with a condenser at the top. The heat pipe panel was used in two arrangements, with or without a PV panel above. The heat pipe was able to recover heat via radiation in the case of a non-

covered surface and was able to recover heat and enhance the performance of the PV panel when covered.

Heat pipe heat exchanger system have also been developed by *En Tian* et al. [14]. In this paper, a novel heat pipe heat exchanger was designed in order to recover heat from a flue gas with high particle contents and heat up clean air. To overcome the issue of fouling the heat pipe technology has been applied. The pipes of the system were smoothed in order to avoid fouling and the reduction of cold spots was achieved by the heat pipe as heat pipes are considered isothermal. The system was able to decrease by 15% the natural gas consumption of the whole system. *K.Wang* et al [15] investigated the heat transfer characteristics, energy and exergy performance a coil type solar dish receiver. The solar efficiency of the receiver was above 58%. The irradiance reached to almost 650 W/m^2.

Heat pipes have also been widely investigated in solar collector applications using radiation heat transfer. This type of heat pipe system is used to warm up water for district and domestic heating. *Chougule* et al. [16] investigated the use of heat pipe with different working fluids (pure water, water-surfactant and CNT-water) for different flow rates and angles. Similarly, *Boris Rassemakn* et al. [17] investigated the use of an aluminium heat pipe applied to solar collectors. The heat pipe made of aluminium was placed on a roof in order to recover heat from solar radiation.

The use of heat pipe systems in the ceramics industry is quite limited while the possible application of the technology is broad. The development of a novel radiative heat pipe to recover heat and improve the cooling profile of the tiles has not been investigated yet.

3. Experimental setup

3.1. Heat pipe system

The radiative heat pipe system is composed of ten parallel pipes of 28 mm diameter and 2 mm wall thickness connected together via a bottom pipe, also of 28 mm diameter, and a condenser section. The condenser section is a shell and tube system where the coolant flows through nine pipes of diameter 10 mm and wall thickness 1 mm Fig. 7.

The length of the evaporator section is 430 mm with an inclination of 5° (see Fig. 8). Each adiabatic section is composed of an
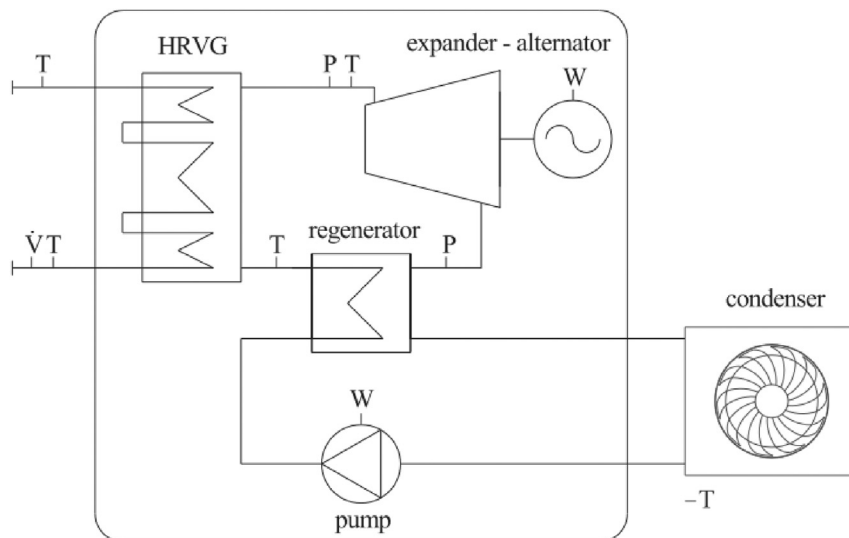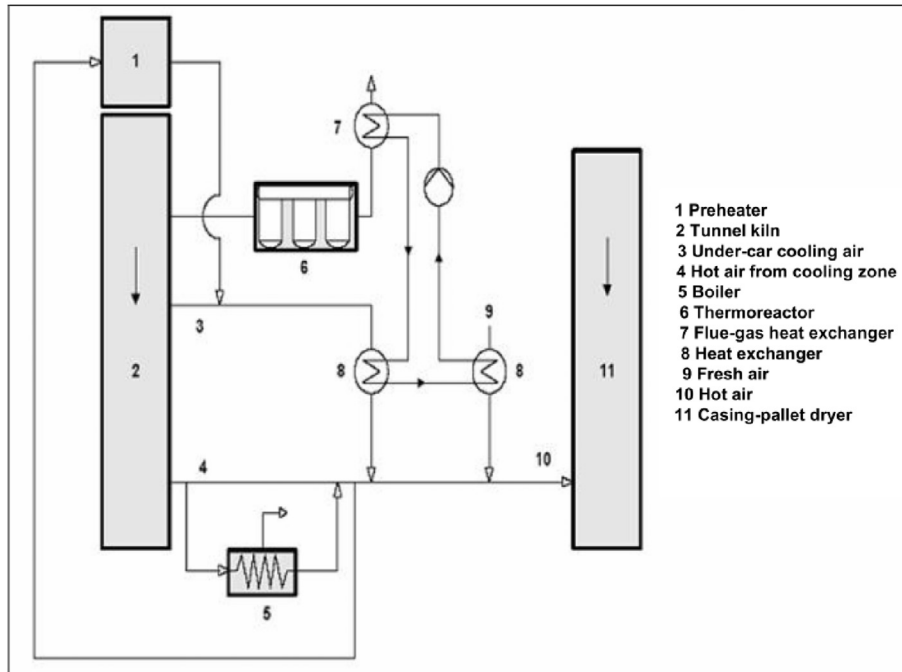

Fig. 4. Schematic of an ORC [7].

Fig. 5. Schematic view of a combined heat recycling system [4].
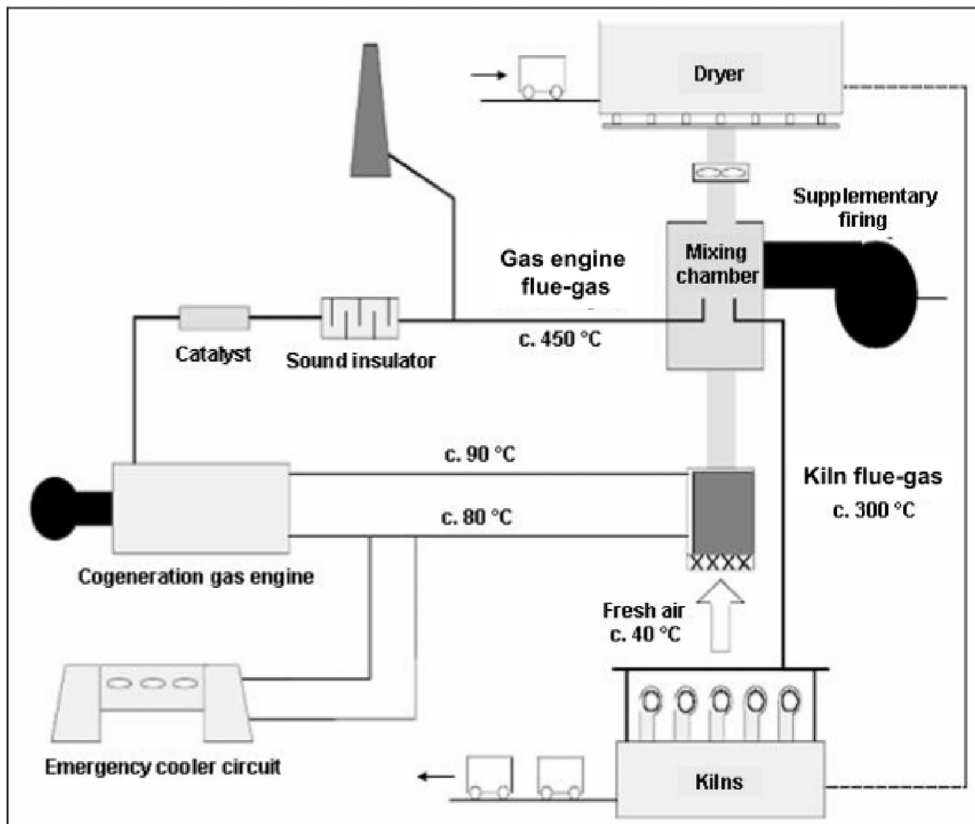

Fig. 6. Schematic of hot air generation using cogeneration system [4].

elbow and two straight pipes for each individual horizontal pipe. The whole system was welded together using TIG welding in order to match the design pressure of 100 bars. In order to protect the integrity of the heat pipe, a rupture disc has been installed at the top of the condenser section.

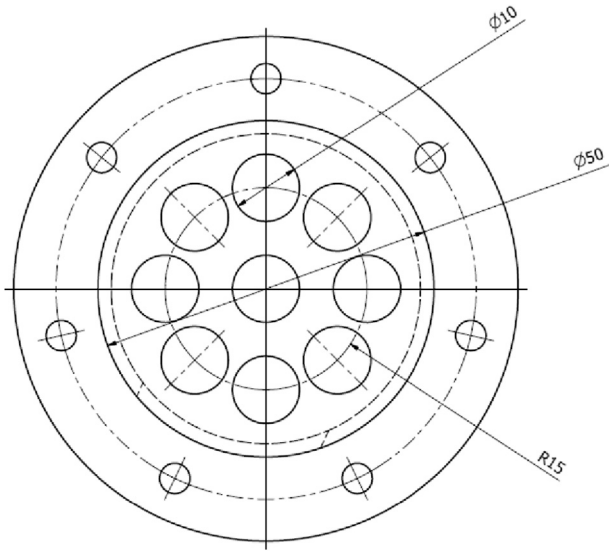The radiative heat pipe is made of stainless steel 304. The
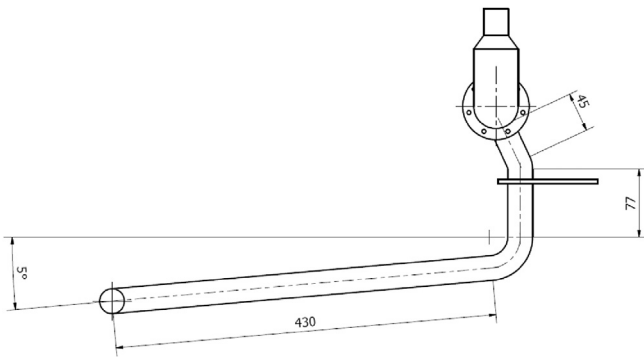
Fig. 7. Condenser drawing side view.

Fig. 8. Radiative heat pipe side view.

distance between each tube is 15 mm.

The radiative heat pipe was placed in a kiln to test the radiative and natural convection heat transfer capacity at different water flow rates and different heater temperatures (see Fig. 9). The kiln is made of insulation material for high temperatures. The surface area of the heater was 0.25 m² and, to be as close as possible to the emissivity of the tiles, the selected heater was made of ceramic heater pads. The maximum capacity of the heater was 7 kW.

3.2. Cooling system and instrumentation

The cooling system of the heat pipe was composed of an open loop water cooling system (see Fig. 10). The pump was drawing the water from the main supply tank trough the condensing tubes welded inside the heat pipe. Then, the water was discarded. Two thermocouples monitored the water side. A flow meter monitored the flowrate.

Eleven mineral insulated K-type thermocouples were welded onto the evaporator section of the radiative heat pipe (see Fig. 11 a and b). The thermocouples were insulated to avoid any error on the thermocouple readings. Two jubilee thermocouples were placed on the condenser section. One thermocouple was welded in a way that the head of the thermocouple was in the heat pipe, so that this thermocouple measured the temperature of the saturated working fluid. The temperatures of the six walls of the kiln were also

Fig. 9. Radiative heat pipe system.

monitored and recorded (see Fig. 11 (c)). Then, two thermocouples were placed in the inlet and outlet of the water cooling system. The water flow rate was recorded using a flowmeter at the inlet of the system and it was controlled using a ball valve. The heater temperature was controlled using a PID system with the temperature of the heater top surface as a set point. When the heater reaches the desired temperature, the PID will switch off the supply in order to tune the heater temperature to the set temperature. Because of the inertia of the heater, the temperature of the heaters will vary from 50 degrees off the set temperatures to 5° after the PID system settles.

3.3. System operation and test plan

The operation of the system was to set the water flow rate as well as the required temperature of the ceramic heaters. The heat pipe will then reach the steady state that depends on the temperatures and flow rate chosen. When the heat pipe is at steady state, the heaters were switched off. In order to record the data, a national instrument data logging system were used. The data logger was composed of two modules, each with 15 thermocouples channels. In order to avoid any noise in the data, the data logger was kept away from the kiln and any computers. The data collected from the experiment were then analysed using Excel in order to manage the large amount of data produced. To calculate the heat recovered from the kiln, it is assumed that the system is at steady state, the fluid properties are constant and the convection heat transfer is constant along the pipes. The specific heat of water at the bulk temperature is 4187 J/kg.K.

The rate of energy transfer for a steady flow of fluid in a pipe can be expressed as

$$\dot{Q} = \dot{m}C_p(T_e - T_i) \tag{1}$$

where:

$\dot{Q}$: Rate of heat transferred to the heat sink.
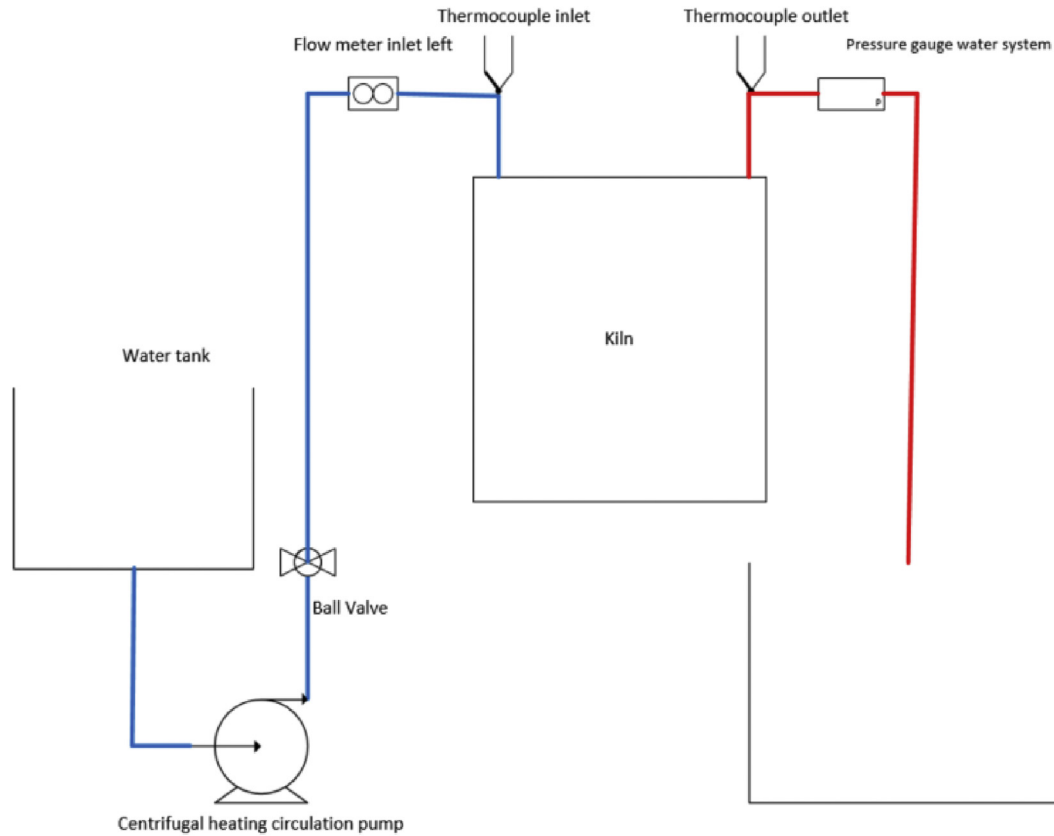$\dot{m}$: Mass flow rate going through the condenser.

Fig. 10. Heat pipe cooling system.

C_p: Specific heat of the water at 20 °C (J/kg.K).
T_e: Temperature at the outlet of the condenser (°C).
T_i: Temperature at the inlet of the condenser (°C).

The tests carried out during the session are summarised in the table below.

parallel tubes and the bottom collector. The saturated vapour then flows upwards to the condenser section [18]. Then the vapour rejects the latent heat at the condenser by condensation and flows back to the evaporator section as shown in Fig. 12. The heat is transferred from the condenser to the cooling fluid via the tube walls by conduction and then by forced convection from the inner surfaces of the tubes to the cooling fluid.

Dream Test 25% working fluid				
Ceramics temp (deg)	Flow rate (L/min)			
	5	10	15	20
200	Test 1	Test 2	Test 3	Test 13
300	Test 4	Test 5	Test 6	Test 14
400	Test 7	Test 8	Test 9	Test 15
500	Test 10	Test 11	Test 12	Test 16

4. Theoretical model of the heat transfer

The heat pipe heat exchanger is based on two-phase heat transfer to transport the heat from the kiln to the coolant. The heaters in the kiln emit the heat to the heat pipe and the walls and the top wall of the kiln. In addition, heat is transferred from the heaters to the air by natural convection. The evaporator section of the heat pipe absorbs the heat from the heaters and the walls by radiation, as well as from the hot air by natural convection. The heat is then transferred through the heat pipe walls by conduction to the inner surface of the heat pipe evaporator section.

The working fluid contained in the heat pipe evaporates in the

The thermal modelling of the system is carried out by applying the electrical network analogy approach, where each thermal resistance is considered to be an electrical resistance and the heat transfer rate is the current passing through the resistances. The thermal network model of the system is presented in Fig. 13.

The temperature symbols presented in Fig. 13 are:

T_{air}: Air temperature in the kiln (K)
T_{heater}: Heater temperature in the kiln (K)
T_{eo}: Temperature of the evaporator outer wall (K)
T_{ei}: Temperature of the internal wall of the evaporator (K)
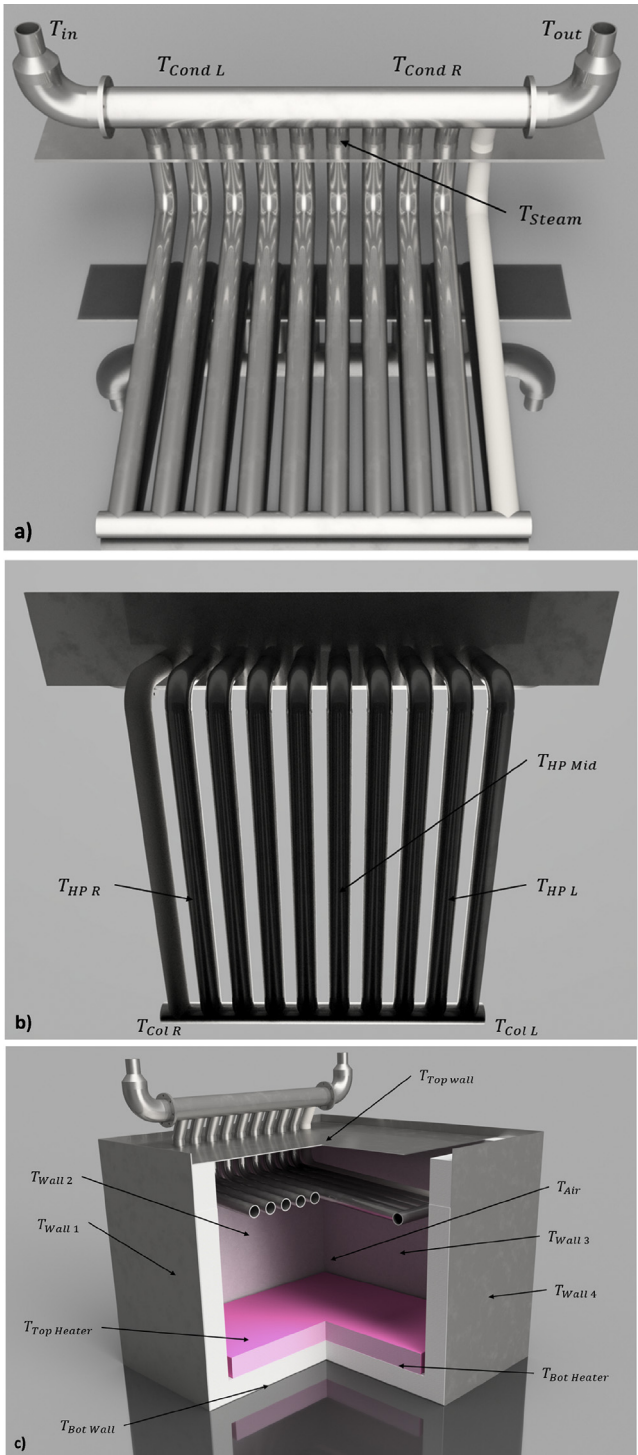T_v: Temperature of the vapour in the adiabatic section (K)

Fig. 11. Thermocouple locations.

T_{co}: Temperature of the outer wall of the condenser (K)
T_{ci}: Temperature of the internal wall of the condenser (K)
T_{cold}: Temperature of the water coolant (K)

The resistance symbols are:

$R_{N.convection}$: Thermal resistance of natural convection (K/W)
R_{rad}: The resistance of heat transfer by radiation (K/W)

R_{cond_e}: Conduction thermal resistance through the evaporator wall (K/W)
R_{ei}: Thermal resistance of boiling heat transfer (K/W)
R_{ci}: Condensation heat transfer at the condenser section (K/W)
R_{cond_c}: Conduction thermal resistance through the condenser wall (K/W)
R_{co}: Convection Thermal resistance of forced convection from the condenser wall to the coolant (K/W)
R_{HP}: Heat pipe thermal resistance (K/W)

The heat transfer rate through the heat pipe can be determined from the following equation

$$Q = Q_{Natural\ convection} + Q_{radiation} \tag{2}$$

where:

Q: Overall heat transfer rate (W)
$Q_{Natural\ convection}$: Heat transfer rate between the heat pipe and the air in the kiln by natural convection (W)
$Q_{radiation}$: Heat transfer rate between the heat pipe and the kiln by radiation (W)

The rate of heat transfer through the heat pipe can be calculated through the following equations:

$$Q = \frac{T_{eo} - T_{ci}}{R_{HP}} = \frac{\frac{T_{water,\ out} - T_{water,\ in}}{\ln\left(\frac{T_{ci} - T_{water,\ in}}{T_{ci} - T_{water,\ out}}\right)}}{R_{co}} \tag{3}$$

where:

$$R_{HP} = R_{cond,\ e} + R_{ei} + R_{ci} + R_{cond,\ c} \tag{4}$$

The heat transfer by natural convection can be calculated as follow:

$$Q_{Natural\ convection} = \frac{T_{air} - T_{eo}}{R_{N.convection}} \tag{5}$$

where:

T_{air}: Air temperature in the kiln (K)
T_{eo}: Temperature of the evaporator outer wall (K)
$R_{N.convection}$: Thermal resistance of natural convection which can be calculated as follows:

$$R_{N.convection} = \frac{1}{h_{N.convection}.A_{eo}} \tag{6}$$

A_{eo}: Surface area of the external surface of evaporator (m^2)
$h_{N.convection}$: Heat transfer coefficient of heat transfer by natural convection over cylinders which can be calculated from Ref. [19]:

$$h_{N.convection} = \frac{k}{d}\left[0.6 + \frac{0.387Ra^{\frac{1}{6}}}{\left(1 + \left(\frac{0.559}{Pr}\right)^{9/16}\right)^{\frac{8}{27}}}\right]^2 \tag{7}$$

k: Thermal conductivity of air (W/m K)
d: Pipe diameter (m)
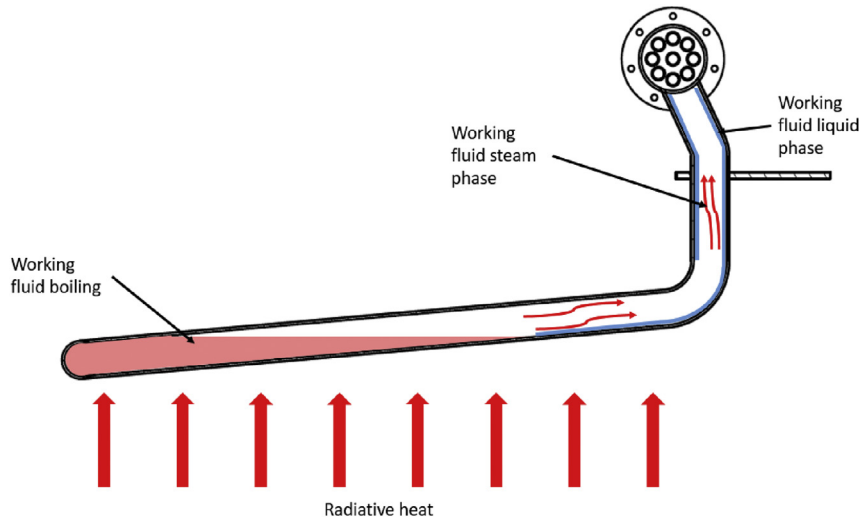Pr: Prandtl number
Ra: Rayleigh number

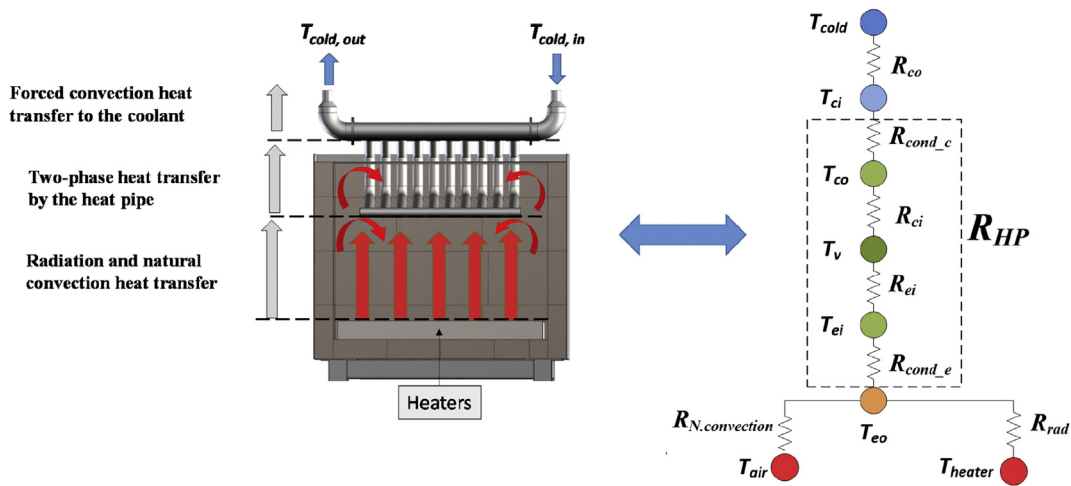**Fig. 12.** Schematic of the Boiling and condensation in the heat pipe.

Fig. 13. Thermal model of the heat transfer in the kiln by the HP system.

The heat transfer by radiation can be calculated as follows:

$$Q_{radiation} = \frac{T_{heater} - T_{eo}}{R_{radiation}} \quad (8)$$

T_{heater}: Heater temperature in the kiln (K)
T_{eo}: Temperature of the evaporator outer wall (K)

The radiation heat transfer was determined through the following analysis. The heaters radiate heat to the heat pipe and to the walls of the kiln. Since the kiln is insulated, the walls receive heat from the heaters and reradiate the heat in all directions to the heaters and the heat pipe. The heat transferred by radiation in the kiln is represented in Fig. 14. The thermal resistance between the walls depends on the view factor and the surface area. However, as the kiln is fully insulated, the thermal model of the heat transfer by radiation can be simplified as shown in Fig. 15.

It was assumed in the thermal model that all the surfaces are grey, opaque, and diffuse.

The symbols used in the figures are:

E_H : Emitted heat from the heater surface (W/m^2)
J_H: Radiosity of the heaters surface which is the overall radiation leaving the heater surface (W/m^2)
J_{HP}: Radiosity of the heat pipe which is the overall radiation leaving the heat pipe surface (W/m^2)
E_{HP}: Emitted heat from the heat pipe surface (W/m^2)
$R_{JH,EH}$: Heater surface resistance to radiation (m^{-2})
$R_{H,W}$: Space resistance to radiation between the heaters and the kiln walls (m^{-2})
$R_{H,HP}$: Space resistance to radiation between heaters and the heat pipe surface (m^{-2})
$R_{W,HP}$: Space resistance to radiation between kiln walls and the heat pipe surface (m^{-2})
$R_{JHP,EHP}$: Heat pipe surface resistance to radiation (m^{-2})
F_{H-HP}: View factor between the heaters and the heat pipe
F_{H-W}: View factor between the heaters and the walls
F_{W-HP}: View factor between the walls and the heat pipe

Since the radiation is emitted from the heaters to the heat pipe and kiln walls then:
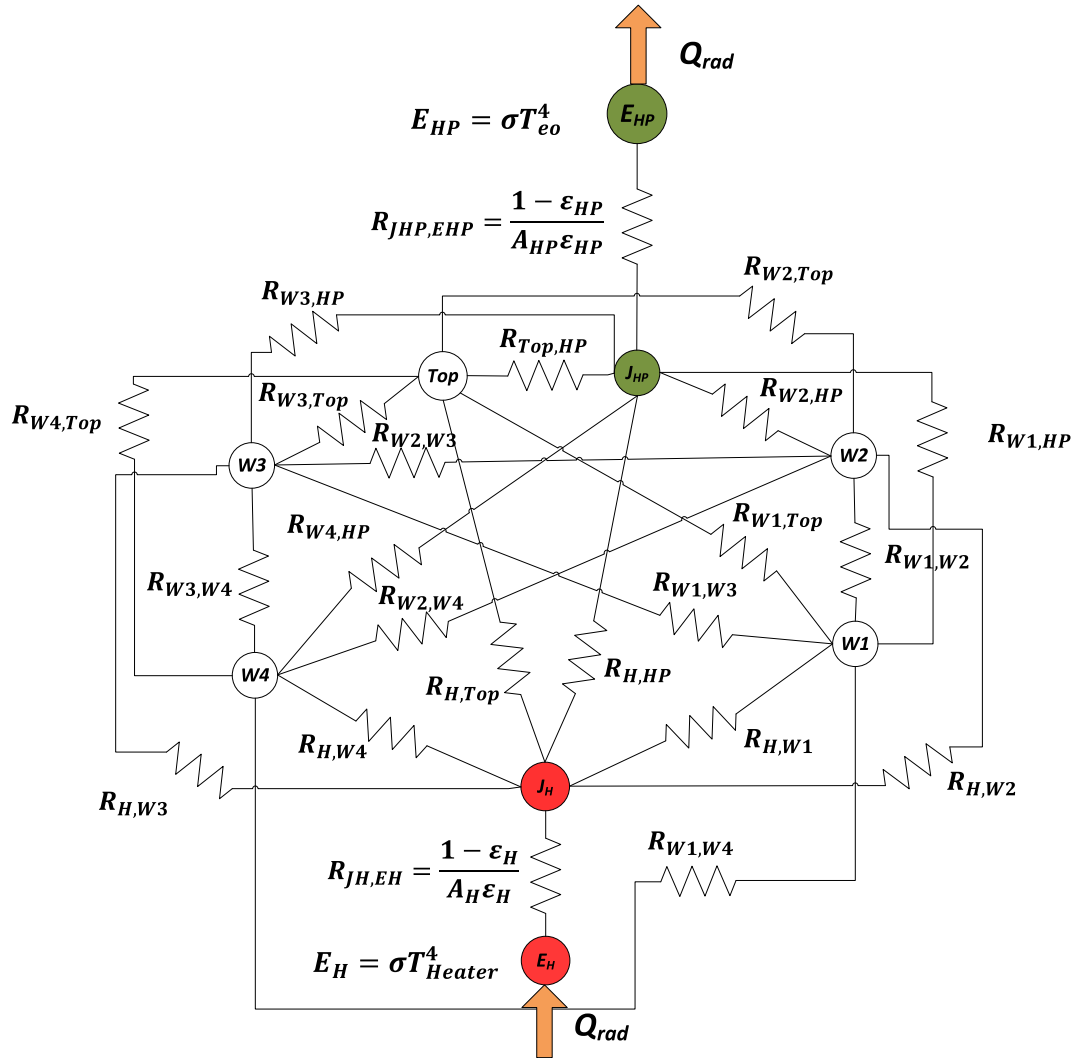
Fig. 14. Thermal model of radiation heat transfer in the kiln.

$$F_{H-HP} + F_{H-W} = 1 \qquad (9)$$

$$F_{H-HP} = 0.271, \quad F_{H-W} = 0.729$$
Hence:

$$Q_{radiation} = \frac{E_H - E_{HP}}{\frac{1-\varepsilon_H}{A_H \varepsilon_H} + \left(A_H F_{H-HP} + \frac{1}{1/(A_H F_{H-W}) + 1/(A_{HP} F_{HP-W})}\right)^{-1} + \frac{1-\varepsilon_{HP}}{A_{HP}\varepsilon_{HP}}} \qquad (10)$$

$$Q_{radiation} = \frac{\sigma\left(T_H^4 - T_{HP}^4\right)}{\frac{1-\varepsilon_H}{A_H \varepsilon_H} + \left(A_H F_{H-HP} + \frac{1}{1/(A_H F_{H-W}) + 1/(A_{HP} F_{HP-W})}\right)^{-1} + \frac{1-\varepsilon_{HP}}{A_{HP}\varepsilon_{HP}}} \qquad (11)$$

where:

ε_H : Emissivity of the heaters
ε_{HP}: Emissivity of the heat pipe
σ: Stephan-Boltzmann constant; 5.67×10^{-8} W/m^{2}K^4

5. Results and discussion

5.1. Results

The tests were conducted for four heater surface temperatures and four different cooling water flow rates. The first test was with a set point at 400 °C. Fig. 16 shows the temperature difference between the inlet and outlet of the water cooling system for the four flow rates and Fig. 16 shows the heat recovered in each case. The heat transferred between the heater and the heat pipe is roughly constant while the temperature difference between the inlet and outlet of the system is changing. The maximum heat recovered of 2100 W was during the test at 20 l/min with ΔT = 1.5 °C. The test at 5 l/min showed the lowest heat recovery of 1700 W at ΔT = 4.8 °C.

During the second test, the heater temperature was set at 500 °C. Fig. 16 shows the ΔT between the inlet and outlet of the radiative heat pipe condenser. The maximum ΔT was 8.4 °C at a flow rate of 5 l/min, the minimum ΔT was 2.0 °C at a flow rate of 20 l/min. The maximum heat transfer was 3100 W at 15 l/min, the minimum was 2900 W for 20 l/min. The heat recovered was approximately constant for the four flow rates. The warm-up of the heat pipe for this heater setting is shown in Fig. 18. The temperature of the heat pipe reaches almost 120 °C for THP 6 and THP 5 before
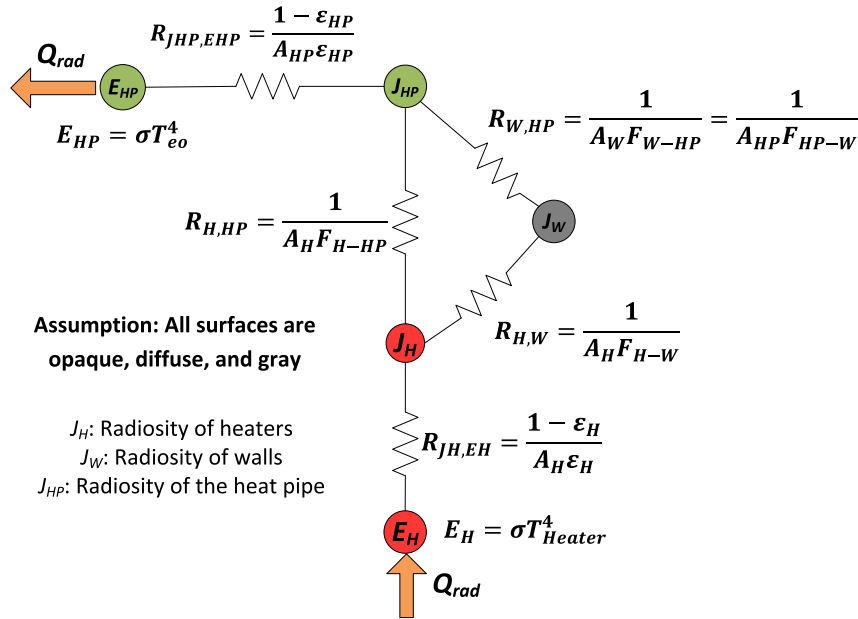
$$R_{JHP,EHP} = \frac{1 - \varepsilon_{HP}}{A_{HP}\varepsilon_{HP}}$$

Q_{rad}

E_{HP}

J_{HP}

$E_{HP} = \sigma T_{eo}^4$

$$R_{W,HP} = \frac{1}{A_W F_{W-HP}} = \frac{1}{A_{HP} F_{HP-W}}$$

J_W

$$R_{H,HP} = \frac{1}{A_H F_{H-HP}}$$

J_H

$$R_{H,W} = \frac{1}{A_H F_{H-W}}$$

Assumption: All surfaces are opaque, diffuse, and gray

J_H: Radiosity of heaters
J_W: Radiosity of walls
J_{HP}: Radiosity of the heat pipe

$$R_{JH,EH} = \frac{1 - \varepsilon_H}{A_H \varepsilon_H}$$

E_H　$E_H = \sigma T_{Heater}^4$

Q_{rad}

Fig. 15. Simplified thermal model of the radiation heat transfer in the kiln.
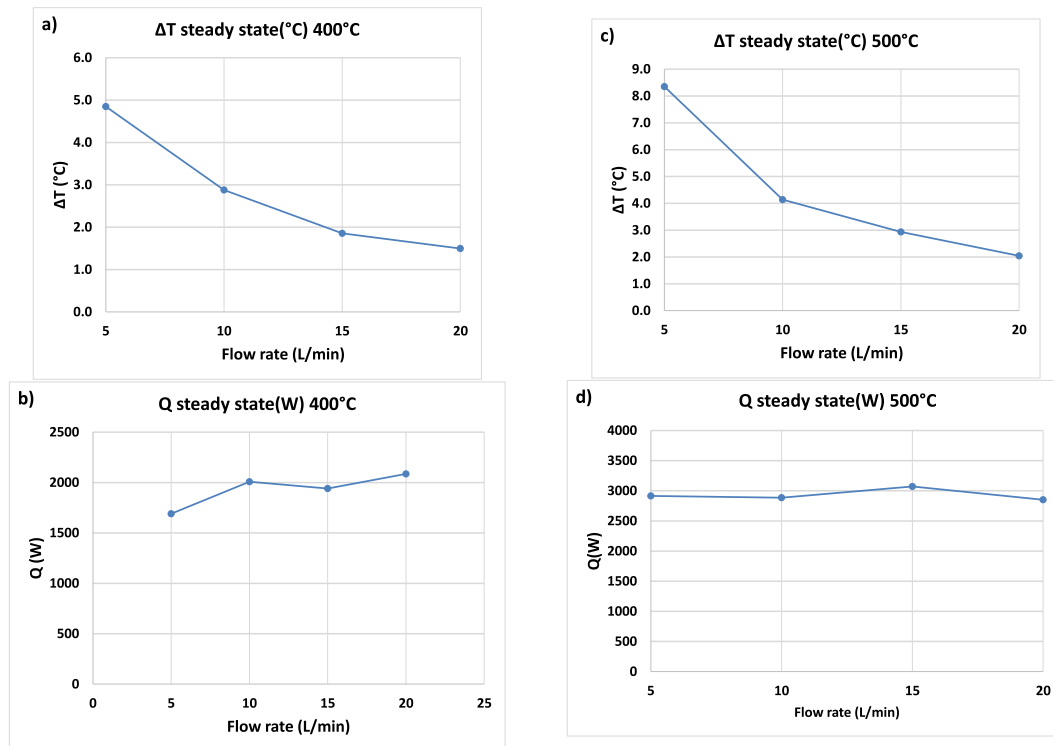
Fig. 16. Results from tests at 400 °C and 500 °C for different water flow rates.

joining the other HP temperatures. This was due to a phenomenon called Geyser boiling [20]. Also, the temperatures recorded by the thermocouples located on the evaporator section of the radiative heat pipe are similar (a maximum variation of 20 °C).

The third test was carried out at a set temperature of 300 °C. The maximum heat recovery was 1200 W at a set flow rate of 20 l/min and the minimum heat recovered was achieved at 1000 W for a flow rate of 5 L/min Fig. 17. (b). The last test was carried out at a set temperature of 200 °C. The maximum heat recovered was 550 W at

a flow rate of 15 l/min and the minimum heat recovered was 400 W for a flow rate of 20 L/min Fig. 17. (d). The temperature of the water inlet and outlet during the fourth test at heater temperature of 200 °C and flow rate of 20 l/min is shown in Fig. 19. The efficiency of a system can be defined as the energy output divided by the energy input in the system, then, the average heat pipe efficiency at a set temperature of 500 °C was 42%. The energy efficiency of the system for a set point of 400 °C was 26%. These figures apply if the heater is constantly providing 7 kW. However, the heaters were controlled
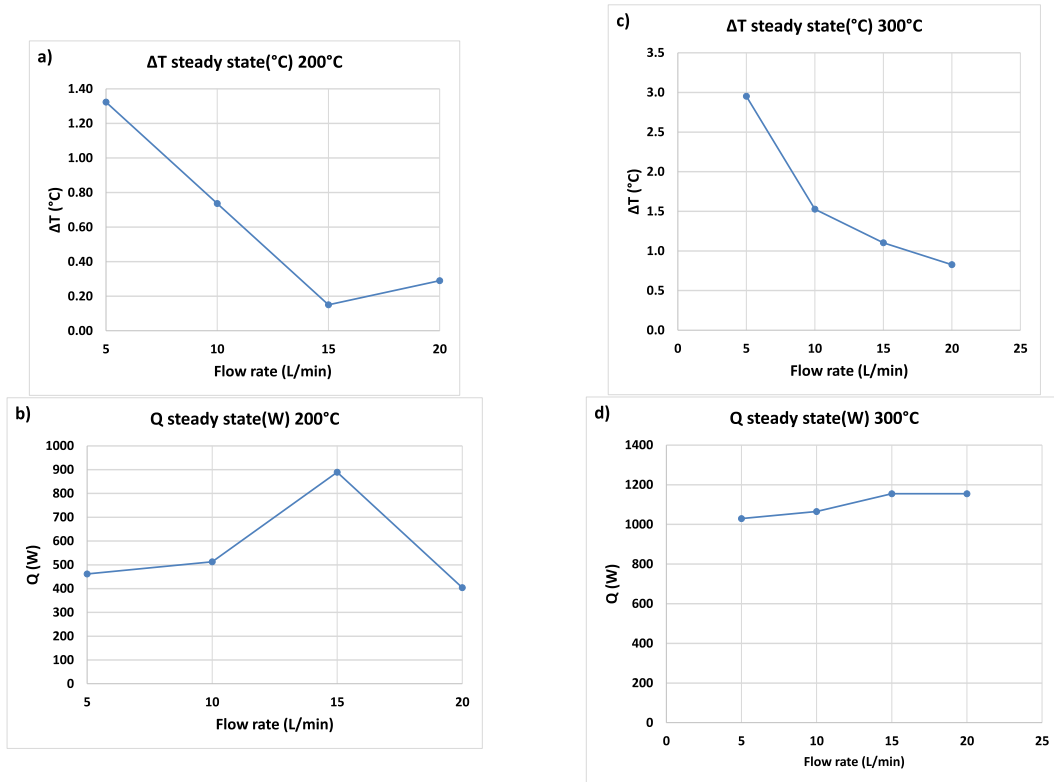
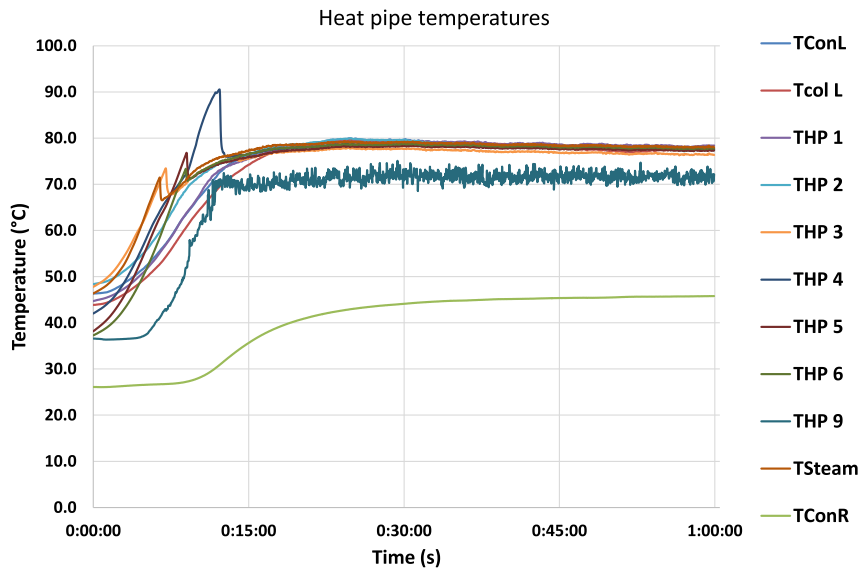Fig. 17. Results from tests at 300 °C and 200 °C for different water flow rates.

Fig. 18. Heat pipe temperatures 500 °C 5 L/min test.

by a PID, which switched on and off to maintain the set point temperature. In later stages, an energy logger will be installed to measure the energy input in the system and compare it with the energy recovered at steady state. Using this method, the efficiency of the system can be calculated more accurately. In addition, the insulation at the bottom of the kiln can be improved to decrease the heat loss via conduction thus increasing the thermal efficiency of the system.

Fig. 20 represents the heat recovered depending on the heat

source temperature set point and the flow rates. The modification of the flow rates does not impact greatly on the heat recovered by the heat pipe system.

5.2. Theoretical results

The heat transfer rate from the kiln to the heat pipe was calculated theoretically by combining the radiation and convection heat transfer rates according to the approach given in the
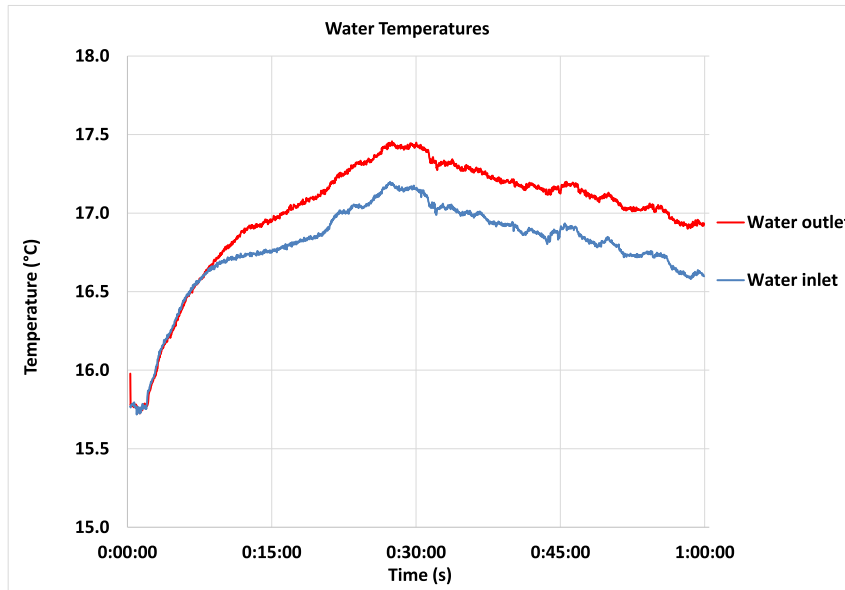
Fig. 19. Outlet/inlet temperatures water 200 °C 20 L/min test.

theoretical modelling section. The theoretical results of the heat transfer rate versus the heater temperature are presented in Figs. 21–24. It can be noted from the figures that the heat transfer rate by natural convection was higher than the heat transfer by radiation at a heater temperature of 200 °C. As the heater temperature increased, the radiation heat transfer increased significantly in comparison to natural convection heat transfer. At the heater temperature of 500 °C and water flow rate of 5 l/min, the radiation heat transfer rate was 223% higher than natural convection heat transfer. At the same heater temperature and higher water flow rates, the radiation heat transfer rate was 155% higher than natural convection heat transfer. It can also be noted that the water flow rate has no change on the radiation heat transfer rate, while the natural convection heat transfer rate was affected by changing the water flow rate. This can be explained by the fact that natural convection heat transfer coefficient depends on the temperature difference between the air and the heat pipe evaporator surface. In addition, the heat pipe surface temperature and the air temperature were not the same among all of the tests. This was due
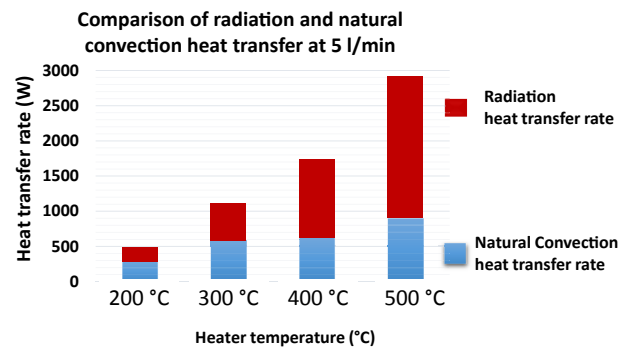

Fig. 21. Theoretical natural convection and radiation heat transfer rate at water flow rate 5 l/min.

to the energy balance between the heat input from the heaters, the heat transfer rate by the heat pipe, and the heat losses from the kiln
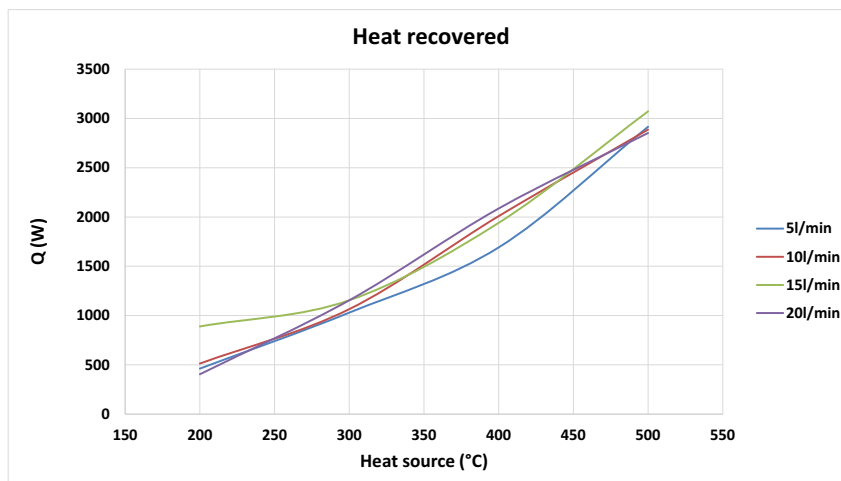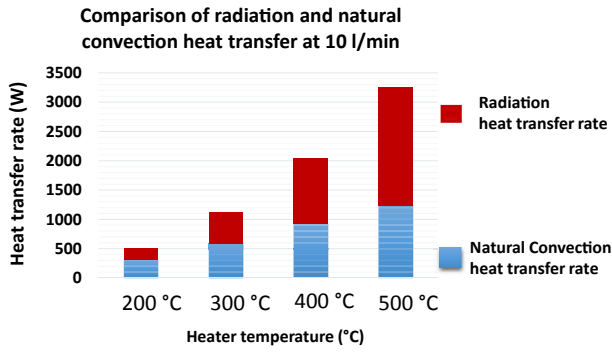

Fig. 20. Heat recovered.

Comparison of radiation and natural convection heat transfer at 10 l/min

Fig. 22. Theoretical natural convection and radiation heat transfer rate at 10 l/min.

Comparison of radiation and natural convection heat transfer at 15 l/min
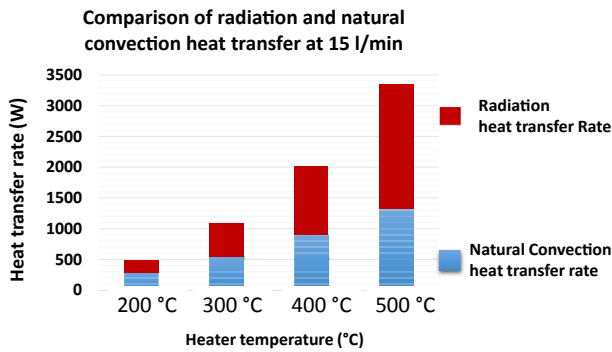
Fig. 23. Theoretical natural convection and radiation heat transfer rate at 15 l/min.

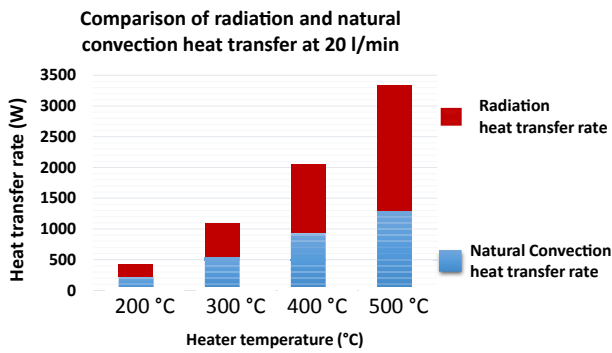## Comparison of radiation and natural convection heat transfer at 20 l/min

Fig. 24. Theoretical natural convection and radiation heat transfer rate at 20 l/min.

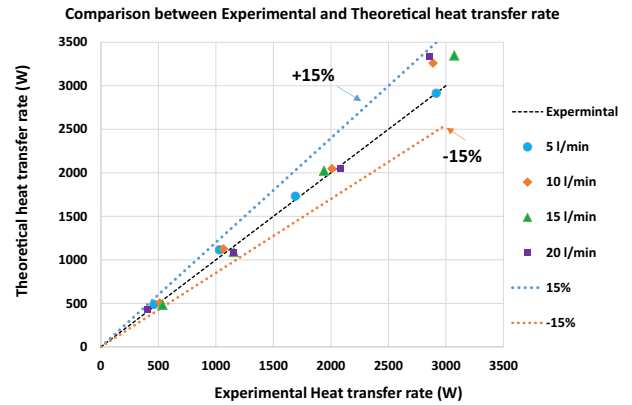## Comparison between Experimental and Theoretical heat transfer rate

Fig. 25. Comparison between the theoretical and experimental heat transfer rate.

issues can influence the results of the experiment. In order to mitigate the error of the system, an error analysis have been carried out. For the radiative heat pipe, Q_{in} and Q_{out} values can be defined. If the system is perfectly insulated then, $Q_{in} = Q_{out}$. Electric heaters were used to warm up the heat pipe, Q_{in} is defined to equal to 7 kW. No power logger was installed during the experiment at this stage, the maximum power used during the test will be defined for the error analyses. Q_{out} is defined as

$$Q_{out} = \dot{m}C_p \Delta T = \dot{V}\rho C_p \Delta T \tag{12}$$

where

$$\Delta T = T_{out} - T_{in} \tag{13}$$

Q_{out} : Rate of heat transferred to the heat sink.
$\dot{V}$: Volume of water going through the tube bundle.
ρ: Density of water at the average temperature (kg/m^3).
C_p: Specific heat of the water at the average temperature (J/kg.K).
T_{out}: Temperature at the outlet of the condenser (°C).
T_{in}: Temperature at the inlet of the condenser (°C).

The variables used to calculated the heat recovered may or may not have any associated errors, these uncertainties are detailed in

to the surroundings in the lab.

The theoretical results of the overall heat transfer rate in the kiln are compared with the experimental results in Fig. 25. Fig. 25 presents the theoretical and experimental results for the tests conducted at various heater temperatures and water flow rates from 5 l/min to 20 l/min. It can be seen that the theoretical results using the theoretical approach presented has an excellent agreement with the experimental results with less than 15% error.

5.3. Error analysis

Error in experimental procedures can be impacted by different factors such as human error, inaccurate experiment, location of the data logging equipment, age of the thermocouples, etc. and these

Variable	Read from	Associated error
T_{out}	National instrument PXIe-1071-9213	**K/T Type:** ±0.02 °C 0.03% error between −210 °C and 760 °C ±0.02 °C 0.03% error between −270 °C and 1260 °C
T_{in}	National instrument PXIe-1071-9213	**K/T Type:** ±0.02 °C 0.03% error between −210 °C and 760 °C ±0.02 °C 0.03% error between −270 °C and 1260 °C
$\dot{V}$	Gems Sensors RotorFlow Electronic Flow Sensor	6.0–45.0 l/min ±7% 15.0–75.0 l/min ±15%
C_p	Value based on T_{out} and T_{in}	Ignore
ρ	Value based on T_{out} and T_{in}	Ignore

Each variable has an error associated with it, these errors are calculated using the following equations;

Variable	Equation	Associated error
ΔT	$\Delta T = T_{out} - T_{in}$	$S_{\Delta T} = \sqrt{S_{tout}{}^2 + S_{tin}{}^2}$
$T_{w\,av}$	$T_{w\,av} = \dfrac{T_{out} + T_{in}}{2}$	$S_{\Delta T} = \sqrt{S_{tout}{}^2 + S_{tin}{}^2}$
Q_{out}	$Q_{out} = \dot{m}C_p\Delta T = \dot{V}\rho C_p\Delta T$	$S_{Qout} = Q_{out}\sqrt{\left(\dfrac{S_V}{V}\right)^2 + \left(\dfrac{S_{\Delta T}}{\Delta T}\right)^2}$

The results of the error analysis have been summarised in the following table.

	Tin	Tout	V	Q	ΔT	Associated error to Q
Test 1	11.1	12.5	5	474.5	1.4	7.39%
Test 2	12.9	13.6	10	513.1	0.7	8.51%
Test 3	17.8	18.6	15	889.6	0.8	8.32%
Test 13	16.9	17.1	20	404	0.2	19.08%
Test 4	15.5	18.5	5	1029.5	3	7.10%
Test 5	13.7	15.2	10	1062.7	1.5	7.37%
Test 6	13.6	14.7	15	1154	1.1	7.66%
Test 14	13.1	13.9	20	1155.3	0.8	8.19%
Test 7	10.2	14.7	5	1572.5	4.5	7.04%
Test 8	9.7	12.5	10	1971.3	2.8	7.10%
Test 9	13	14.8	15	1908	1.8	7.25%
Test 15	13.2	14.4	20	1692.5	1.2	7.56%
Test 10	10.4	17.3	5	2435.1	6.9	7.02%
Test 11	12.3	15.4	10	2134	3.1	7.09%
Test 12	10.7	12.6	15	2078.3	1.9	7.22%
Test 16	4.5	5.8	20	1860.4	1.3	7.38%

Most of the results of the error analysis are between 8% and 7%, which is acceptable, apart from those from test 13. This can be explained by the high flow rate of the water in the flowmeter, the low heat recovery and hence the small temperature difference. The uncertainties in flow rate and temperature difference generate a maximum error of 77 W for a total heat recovery of only 404 W.

6. Conclusion

A novel radiative heat pipe to recover heat from ceramic tiles has been designed and tested. The thermal performance of the radiative has been heat pipe investigated experimentally in a lab scale kiln. The heat transfer from the kiln to heat pipe has been conducted theoretically also.

- The effect of the heaters temperature in the kiln and the water flow rate on the thermal performance of the heat pipe has been investigated.
- The heat pipe was able to recover between 400 W and 3100 W from the heat source, which had a surface area of 0.261 m^2 depending on the heaters temperature.
- It was observed that the water flow rate did not have a significant role on the amount of heat recovery.
- The theoretical results of the heat transfer in the kiln were compared with the experimental results. The theoretical results comply with the experimental results with an excellent agreement.
- The theoretical model compared evaluated the role of the radiation and natural convection heater transfer on the overall heat transfer to the heat pipe. The heat transfer rate by natural convection was important at heaters temperature of 200 °C while the radiation was the dominant at higher temperatures.
- The results presented in this paper validated the possibility of recovering heat via radiation and natural convection in an enclosed kiln.
- The heat recovered from the heat pipe system can be applied in an industrial scale to warm up a heat carrier fluid to the dryer or spray dryer.
- The error analysis has shown a good accuracy in the results with an average error (excluding the error analyse of test 13) of 7.5%.

The design system proved to be able to recover large amount of heat in a ceramic kiln. The potential for heat recovery in the ceramics manufacturing sector is substantial. The heat pipe system will be able to fit in a roller earth ceramics kiln, replacing the current system.

As discussed above, heat pipe system using radiation heat recovery have been instigated by *Jouahra* et al. [12]. The heat pipe system managed to recover up to 15.6 kW. The presented system managed to recover, in a different scale up to 4 kW. The potential for the heat pipe technology in waste heat recovery using tradition is important and should be investigated father with different type of heat source and industry.

References

[1] Olabi AG. Energy quadrilemma and the future of renewable energy. Energy 2016;108:1–6. https://doi.org/10.1016/J.ENERGY.2016.07.145.
[2] Jouhara H, Olabi AG. Editorial: industrial waste heat recovery. Energy 2018;160:1–2. https://doi.org/10.1016/j.energy.2018.07.013.
[3] Ceramics-unie. Ceramic Unie facts and figures. 2017. http://cerameunie.eu/ceramic-industry/facts-figures/. [Accessed 20 December 2017].
[4] European Comission. Reference document on best available techniques in the ceramic manufacturing industry. 2007. p. 210–1.
[5] Agrafiotis C, Tsoutsos T. Energy saving technologies in the European ceramic sector: a systematic review. Appl Therm Eng 2001;21:1231–49. https://doi.org/10.1016/S1359-4311(01)00006-0.
[6] Anonymous. Industrial microwave drying makes the breakthrough, vol. 5; 1995. p. 230–1.
[7] Peris B, Navarro-Esbrí J, Molés F, Mota-Babiloni A. Experimental study of an ORC (organic Rankine cycle) for low grade waste heat recovery in a ceramic industry. Energy 2015;85:534–42. https://doi.org/10.1016/j.energy.2015.03.065.
[8] Mezquita A, Boix J, Monfort E, Mallol G. Energy saving in ceramic tile kilns: cooling gas heat recovery. Appl Therm Eng 2014;65:102–10. https://doi.org/10.1016/j.applthermaleng.2014.01.002.
[9] Beltran J. Cogeneration systems in the ceramics tile sector. In: Proceedings of the workshop on new technologies for the rational use of energy in the ceramics tiles industry, DG for Ene, EC, Castellon de la Plana, Spain; 1994.
[10] Rentz O, Schmittinger A, Jochum R, Schultmann F. Exemplary investigation into the state of practical realisation of integrated environmental protection within the ceramics industry under observance of the IPPC-directive and the development of BAT reference documents. French- German Institute for Environ; 2001. p. 44–52.
[11] Delpech B, Milani M, Montorsi L, Boscardin D, Chauhan A, Almahmoud S, Axcell B, Jouhara H. Energy efficiency enhancement and waste heat recovery in industrial processes by means of the heat pipe technology: case of the ceramic industry. Energy 2018;158:656–65. https://doi.org/10.1016/j.energy.2018.06.041.
[12] Jouhara H, Almahmoud S, Chauhan A, Delpech B, Nannou T, Tassou SA, Llera R, Lago F, Arribas JJ. Experimental investigation on a flat heat pipe heat exchanger for waste heat recovery in steel industry. Energy Procedia 2017;123:329–34. https://doi.org/10.1016/j.egypro.2017.07.262.
[13] Jouhara H, Milko J, Danielewicz J, Sayegh M a, Szulgowska-Zgrzywa M, Ramos JB, Lester SP. The performance of a novel heat pipe based thermal and PV/T (photovoltaic and thermal systems) solar collector that can be used as an energy-active building envelope material. Energy 2015:1–7. https://doi.org/10.1016/j.energy.2015.07.063.

[14] Tian E, He Y-L, Tao W-Q. Research on a new type waste heat recovery gravity heat pipe exchanger. Appl Energy 2017;188:586–94. https://doi.org/10.1016/j.apenergy.2016.12.029.

[15] Wang K, Wu H, Wang D, Wang Y, Tong Z, Lin F, Olabi AG. ScienceDirect Experimental study on a coiled tube solar receiver under variable solar radiation condition, vol. 122; 2015. p. 1080–90. https://doi.org/10.1016/j.solener.2015.10.004.

[16] Chougule SS, Sahu SK, Pise AT. Frontiers in Heat Pipes performance enhancement of two phase thermosyphon flat-plate solar collectors by using surfactant and. 2013. p. 1–6. https://doi.org/10.5098/fhp.v4.1.3002. 013002.

[17] Rassamakin B, Khairnasov S, Zaripov V, Rassamakin A, Alforova O. Aluminum heat pipes applied in solar collectors. Sol Energy 2013;94:145–54. https://doi.org/10.1016/j.solener.2013.04.031.

[18] Jouhara H, Chauhan A, Nannou T, Almahmoud S, Delpech B, Wrobel LC. Heat pipe based systems - advances and applications. Energy 2017;128:729–54. https://doi.org/10.1016/j.energy.2017.04.028.

[19] Cengel Y a, Klein S, Beckman W. Heat transfer: a practical approach. 2002.

[20] Tecchio C, Oliveira JLG, Paiva KV, Mantelli MBH, Galdolfi R, Ribeiro LGS. Geyser boiling phenomenon in two-phase closed loop-thermosyphons. Int J Heat Mass Trans 2017;111:29–40. https://doi.org/10.1016/j.ijheatmasstransfer.2017.03.092.